Electronic interaction between two fluorenyl-bridged molybdenocene dithiolene electroactive centers

K. Youssef, Antoine Vacher, F Barriere, T. Roisnel, Dominique Lorcy

Electronic interaction between two fluorenyl-bridged molybdenocene dithiolene electroactive centers

Khalil Youssef, Antoine Vacher, Frédéric Barrière, Thierry Roisnel, Dominique Lorcy*

Univ Rennes, CNRS, ISCR (Institut des Sciences Chimiques de Rennes) - UMR 6226, F-35000 Rennes, France

Abstract

A bimetallic metal complex involving a fluorene linker between two redox active bis(cyclopentadienyl)molybdenum dithiolene moieties has been synthesized and characterized by electrochemistry and spectroelectrochemistry. Cyclic voltammetry experiments show sequential oxidation of the two redox centers with small ΔE values between the first and the second redox processes and between the third and the fourth ones. Comparative electrochemical studies carried out using either $[NBu_4][PF_6]$ or the poorly coordinating supporting electrolyte $[Na][B(C_6H_4(CF_3)_2)_4]$ in dichloromethane indicate strong electrostatic effects on consecutive electron transfers, especially for highly charged species. Spectroelectrochemical investigations together with DFT calculations evidence that the two molybdenocene dithiolene electrophores are weakly electronically coupled through the organic bridge.

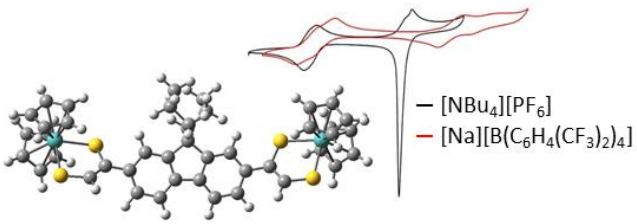

Keywords: Molybdenocene, Dithiolene, bimetallic, electronic coupling, electrostatic interactions

1. Introduction

Metal complexes with non-innocent ligands such as 1,2-dithiolene ligands are promising candidates for the elaboration of either single or multi component conducting molecular materials.[1] The non-innocent character is associated to the redox activity of the ligand and to the electronic delocalization within the MS_2C_2 metallacycle, leading to complexes where the oxidation state of the metal is unclear.[2] More recently, these ligands have also been used for the formation of conducting one- and two-dimensional polymeric materials called coordination nanosheets.[3,4,5,6,7,8] In order to build such polymeric materials, di- and/or tritopic ligands are used with the dithiolene moieties connected by a conjugated organic bridge (Chart 1). Among the few ligands used so far, only planar di- and/or tritopic ligands can be found such as tetrathiooxalate (**tto**),[4,9] 1,2,4,5-benzenetetrathiolate (**btt**),[5,10] benzenehexathiolate (**bht**)[6] or triphenylene hexathiolate (**tpht**).[8] In these ligands, the dithiolene moieties are fused to a conjugated and/or aromatic structure allowing potential electronic communication between the two- or three-coordinated metal ions.[3-8]

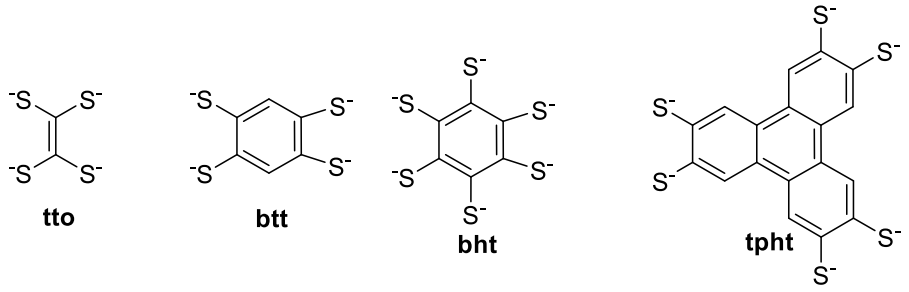

Chart 1. Dithiolene ligands used as precursors of polymeric networks

Among the rare bimetallic complexes using bis(dithiolene) ligands such as **tto** or **btt**, we recently analyzed the electronic interaction between two redox-active bis(cyclopentadienyl) molybdenum dithiolene moieties (Cp_2Mo(dithiolene)) through a phenyl bridge using, either the benzene-1,4-bis(ethylenedithiolate) (**1,4-Ph**) to generate the corresponding complex **$Mo_2$1,4-**

Ph, or the 4,4′-bis(benzenedithiolate) (**bbdt**) to afford **Mo$_2$bbdt** (Chart 2).[11] In order to determine to what extent the length and nature of the organic bridge will allow for electronic interaction, we have investigated here a new bis(dithiolene) ligand involving a fluorene organic linker, which can be viewed as a rigid and planar biphenyl unit. Then, we have studied the formation of the bimetallic complex with two Cp_2Mo(dithiolene) redox active moieties at the 2 and 7 positions of the 9,9-dipropylfluorene moiety to yield **Mo$_2$Flu** (Chart 2). Electrochemical and spectroelectrochemical investigations in the UV-vis-NIR range, evidence the influence of the fluorene linker in **Mo$_2$Flu** *vs* the biphenyl one in **Mo$_2$1,4-bPh** on the electronic interaction between the two metalladithiolene units. DFT calculations have been carried out on bis-molybdenocene dithiolene complexes linked by a fluorenyl, (in **Mo$_2$Flu**), or a biphenyl, (in **Mo$_2$1,4-bPh**) organic bridge to analyze the influence of these linkers with a similar length but a different rigidity. The synthesis of the new bis(dithiolene) ligand and its bis(molybdenocene) complex **Mo$_2$Flu** together with the electrochemical, spectroscopic and theoretical modeling investigations are discussed herein.

Target bis(molybdenocene) complexes

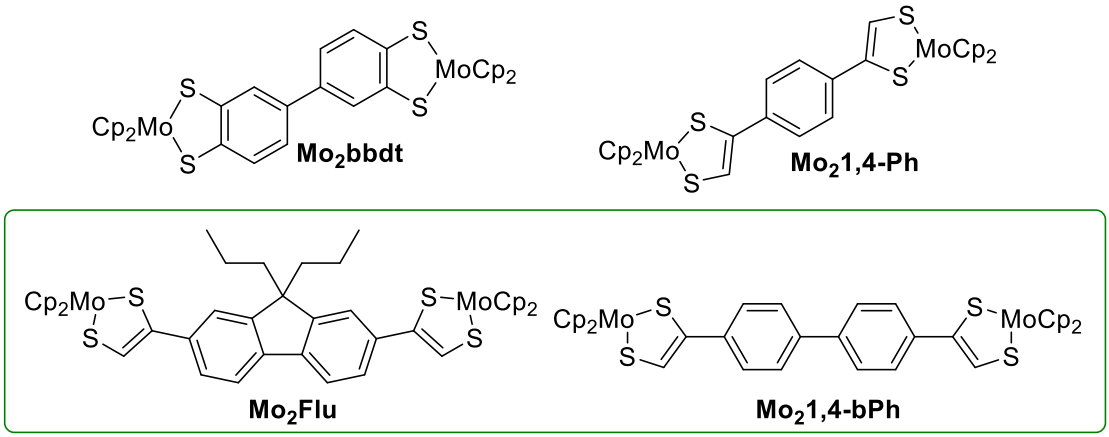

Chart 2. Target bis(molybdenocene) complexes

2. Results and discussion

2.1.Synthesis of the proligand.

Several dithiolene proligands can be used to synthesize the target bimetallic complex: here, we focused our attention on the proligand where the dithiolene is protected by a carbonyl group in a dithiole-2-one heterocycle.[12] The synthetic strategy used to reach this proligand **4** is outlined in Scheme 1. In order to insure the solubility of our bis(ligand), we first inserted on the fluorene core two propyl chains. This was performed by treating fluorene with tBuOK followed by the addition of iodopropane. Then acylation of the fluorene core was realized through the use of acyl chloride in the presence of $AlCl_3$ to generate **2** in 72% yield.[13] Bromination of the two acetyl groups was realized using Br_2 in acetic acid to afford **3**. The 1,1'-(9,9-dipropyl-9H-fluorene-2,7-diyl)bis(2-bromoethan-1-one) **3** was reacted with an excess of potassium isopropyl xanthate and the ring closure was performed in acidic medium to afford the 4,4'-(9,9-dipropyl-9H-fluorene-2,7-diyl)bis(1,3-dithiol-2-one) **4**. This cyclisation into a dithiol-2-one ring has been investigated with two different acids: sulfuric acid or perchloric acid. It is noteworthy that the use of the latter gave a quantitative yield which is almost twice the yield obtained with sulfuric acid (Scheme 1).

Scheme 1

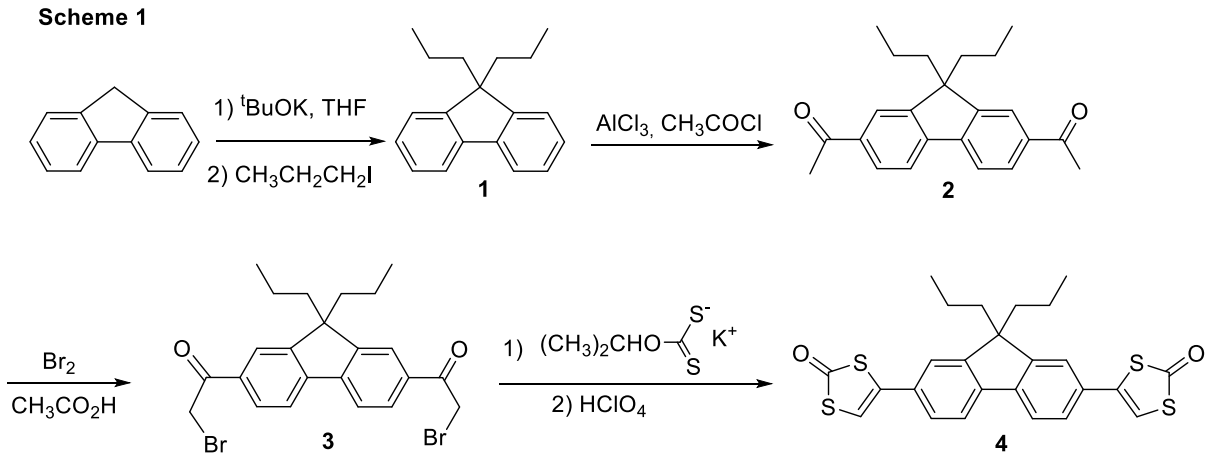

Scheme 1. Synthetic path to the proligand **4**

Crystals of precursors **2**, **3** (see SI, Figures S1 and S2) and the proligand **4** were obtained by slow concentration of their CH_2Cl_2 solution. The molecular structure of **4** is presented in Fig. 1. This proligand is almost planar as the dihedral angles between the dithiol-2-one rings and the fluorene core amount to 9.56° (O1) and 1.73° (O11).

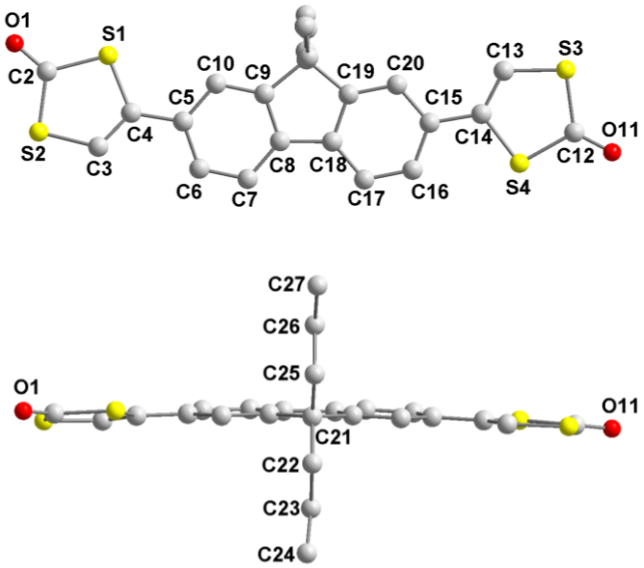

Fig. 1. Molecular structure of proligand **4**. H atoms have been omitted for clarity.

2.2.Synthesis of the complex.

Having in hand this proligand, we conducted the formation of the bimetallic complex, **Mo_2Flu**. Deprotection of both dithiolene units in **4** was performed through the addition of MeONa to a THF solution of **4**. After 2 h at 45 °C, addition of two equivalents of Cp_2MoCl_2 in the medium allowed the synthesis of **Mo_2Flu** in 82 % yield (Scheme 2).

Scheme 2

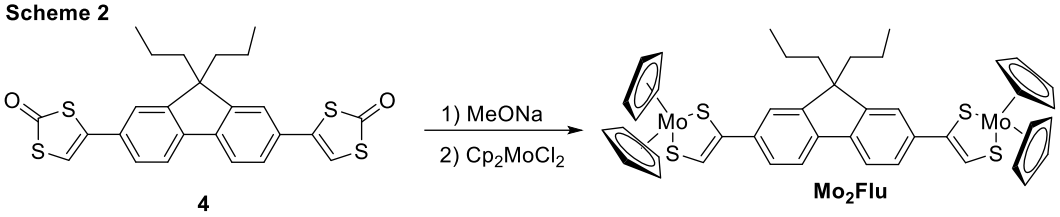

Scheme 2. Synthesis of **Mo_2Flu**.

It should be noted that this compound has the tendency to oxidize easily under air. For instance, the isolated complex left for crystallization into a dichloromethane solution leads to a powder that exhibits a less resolved ^{1}H NMR spectrum. Within electroactive complexes such as Cp_2Mo(dithiolene) complexes, this is often associated with the presence of radical species due to partial oxidation of the molecule. Thus the electrochemical properties of this powder was investigated in CH_2Cl_2 containing Bu_4NPF_6 as supporting electrolyte through voltammetry at a Rotating Disk Electrode (RDE). The resulting RDE voltammogram (Fig. 2) shows indeed that the isolated **Mo_2Flu** complex is a mixture of neutral and oxidized species, in a 83:17 ratio respectively, as determined by the relative limiting current magnitude (I_{limit}^{ox}=2.77µA and I_{limit}^{red} =-0.55µA).

This result was also confirmed by an EPR spectroscopic study of the same powder collected after leaving a dichloromethane solution of **Mo_2Flu** under air. The EPR spectrum of the powder in CH_2Cl_2 at room temperature exhibits an unresolved singlet, as reported before for other Cp_2Mo(dithiolene) complexes.[14,15] This observation is consistent with the RDE voltammogram (Fig. 2) discussed above and hence confirms the presence of a small amount of oxidized Cp_2Mo(dithiolene) complex.

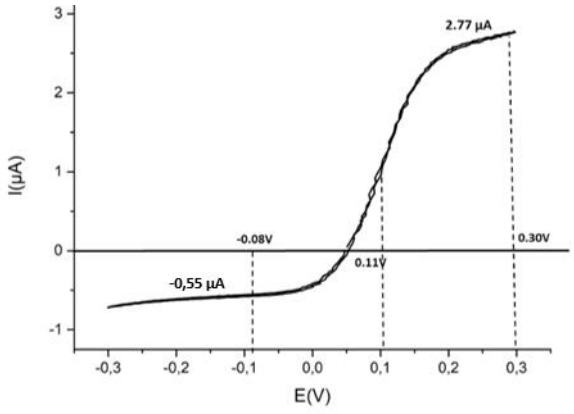

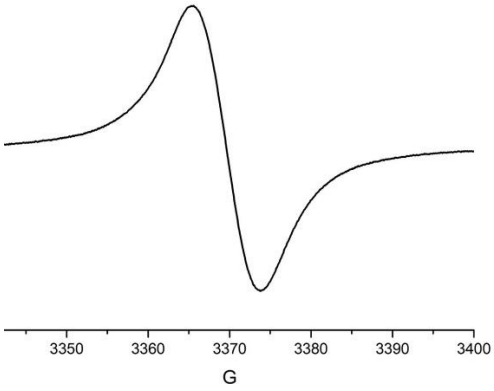

Fig. 2. Investigation of the powder collected after leaving a dichloromethane solution of **Mo_2Flu** under air: (top) Rotating platinum disk electrode voltammogram (10 mV/s, 1500 rpm, 3 mm diameter) of the powder dissolved in CH_2Cl_2/Bu_4NPF_6 0.1 M and (bottom) X-band EPR spectra of the powder in CH_2Cl_2 solution at 298K.

2.3.Electrochemical studies

The electrochemical analyses have been performed on freshly prepared complexes in order to avoid oxidation by air. The redox properties of **Mo_2Flu** have been studied by cyclic voltammetry (CV) and Differential Pulse Voltammetry (DPV), in CH_2Cl_2 in the presence of 0.1 M NBu_4PF_6 as supporting electrolyte (Fig. 3). The oxidation potentials are collected in Table 1 together with the data of analogous complexes **$Mo_2$1,4-Ph** and **Mo_2bbdt** for comparison (Chart 2).[11]

Table 1. Redox potentials[a] of complexes, in CH_2Cl_2 with |Bu_4N][PF_6] 0.1 M (E in V *vs* SCE).

Compound	$E_{1/2}^1$ (ΔEp)[b]	$E_{1/2}^2$(ΔEp)	$E_{1/2}^3$(ΔEp)	Ref
Mo_2Flu	0.06 (60)	0.14(60)	0.83(100)	This work
$Mo_2$1,4-Ph	0.03 (60)	0.19 (60)	0.91 (70)	11
Mo_2bbdt	0.25 (60)	0.37 (60)	1.02 (100)	11

[a] *oxidation processes, taken as the average of the anodic and the cathodic peak potentials.* [b] *ΔE_p (in mV) : peak-to-peak separation.*

Cp_2Mo(dithiolene) moieties are known to be redox active species that can be reversibly and successively oxidized to the cation radical and to the dicationic species.[16] The CV of **Mo₂Flu** shows two main redox processes. A closer look at the first redox process reveals that this system originates from two closely spaced oxidation processes (E^1 = 0.06 V and E^2 = 0.14 V), as confirmed by DPV which has been fitted into two closely spaced redox processes (Fig. 3). The splitting between these two oxidation systems is independent of the concentration of **Mo₂Flu** (between 10^{-2} to 10^{-5} M). This indicates the presence of *intramolecular* interactions between the two Cp_2Mo(dithiolene) units through the organic spacer. At this stage, the present results evidence a stabilization of the cation radical intermediates **Mo₂Flu**$^{+\cdot}$. Then, the oxidation system observed on the CV of **Mo₂Flu** at 0.83 V corresponds to the oxidation of bisoxidized species to the tetracationic system **Mo₂Flu**$^{(4+)}$. Actually, for this last oxidation process, two closely spaced anodic peaks can be also observed on the forward scan of the CV whereas the reverse scan exhibits a cathodic desorption peak which indicates that adsorption has occurred at the electrode upon oxidation to (**Mo₂Flu**)$^{4+}$.

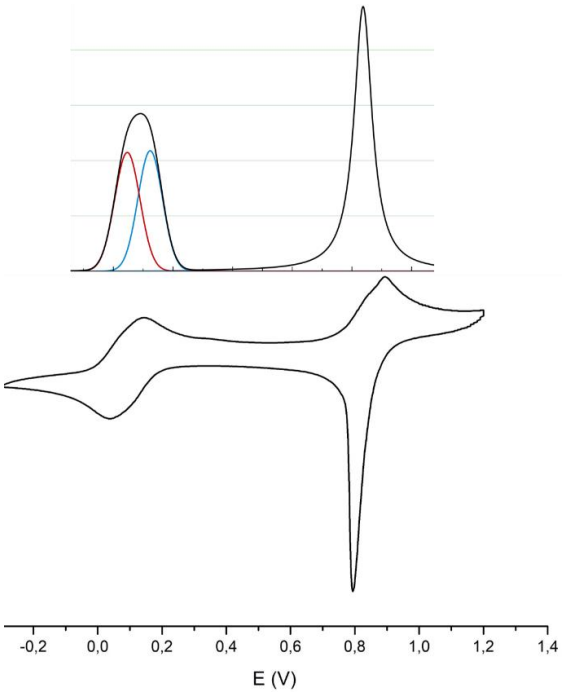

Fig. 3. Cyclic voltammogram (bottom) of **Mo₂Flu** in CH_2Cl_2/[Bu_4N][PF_6] 0.1 M (100 mV/s) together with DPV (5 mV/s) (top), E in V *vs* SCE.

The shape of the **Mo$_2$Flu** CV is similar to that of **Mo$_2$1,4-Ph** and **Mo$_2$bbdt**.[11] The main difference lies with the potential difference between the two first closely-spaced redox processes which amounts to ΔE = 80 mV for **Mo$_2$Flu**, 160 mV for **Mo$_2$1,4-Ph**[11] and 120 mV for **Mo$_2$bbdt**.[11] The fact that the ΔE is halved for **Mo$_2$Flu** when compared with **Mo$_2$1,4-Ph** is associated with its longer fluorenyl organic spacer between the two electrophores compared with the phenyl one. Indeed, the Mo•••Mo distance is 16.06 Å in **Mo$_2$Flu** and 12.65 Å in **Mo$_2$1,4-Ph**. In **Mo$_2$bbdt**, the two phenyl rings of the bridging ligand are fused with the metallacyles which brings the two metallacycles closer than in **Mo$_2$Flu** (Mo•••Mo: 16.06 Å in **Mo$_2$Flu** *vs* 12.75 Å in **Mo$_2$bbdt**, *vide infra*).

Different factors are known to affect the magnitude of the ΔE value between successive one-electron transfers, including electrostatic effects and electronic couplings.[17] In order to get more insights on the electrostatic contribution in the ΔE values we investigated the redox behaviour of **Mo$_2$Flu** in the weakly coordinating electrolyte CH_2Cl_2-[Na][B($C_6H_4(CF_3)_2)_4$] (or [Na][BArF]).[17] The $BArF^-$ anion is known to exhibit a very low ion-pairing strength with positively charged species when used as supporting electrolyte in a low polarity solvent such as dichloromethane, it leads to an increase in ΔE for successive one-electron redox couples due to increased electrostatic interactions between cations generated at the electrode.[17] For comparison, we also studied the reported **Mo$_2$bbdt** complex using the same medium, as this complex exhibits the lowest ΔE value among the two previously reported complexes (**Mo$_2$bbdt** *vs* **Mo$_2$1,4-Ph**). In these conditions, the potential difference between the first two oxidation systems is slightly affected by the nature of the supporting electrolyte, with $\Delta E(E^2 - E^1)$ = 130 mV for **Mo$_2$Flu** (80 mV with Bu_4NPF_6) and ΔE = 200 mV for **Mo$_2$bbdt** (120 mV with Bu_4NPF_6).

It can be noticed also that for both complexes, **Mo$_2$Flu** and **Mo$_2$bbdt**, the third wave is significantly anodically shifted (Fig. 4). For instance, for **Mo$_2$Flu**, the potential difference between the second and the third oxidation system, $\Delta E(E^3 - E^2)$ amounts to 690 mV with Bu_4NPF_6 and reaches 1.0 V with [Na][BArF]. Moreover, the fourth redox system can be now clearly observed on the voltammograms (Fig. 4) with a potential difference with the third one, $\Delta E(E^4 - E^3)$ of 235 mV for **Mo$_2$Flu**. It is worth mentioning that this fourth system could only be distinguished on the forward scan using Bu_4NPF_6 while it is well resolved with [Na][BArF]. Similarly, on the CV of **Mo$_2$bbdt** a fourth redox system can be also observed. However, due to the large anodic shift, this redox system is now located at the limit of the electrolyte potential window. DPV confirmed the presence of this fourth redox system (Fig. 4, bottom). Interestingly, using the fluorinated weakly ion pairing anion $BArF^-$ as supporting electrolyte, no adsorption at the electrode is observed due to the increased solubility of the polycationic species which allows for a better detection of this fourth redox system on the voltammograms in both cases. Indeed, fluorinated weakly coordinating anions, such as the $BArF^-$, increase the solubility of their counter ion in low polarity media like the dichloromethane electrolyte used here and can prevent their adsorption when they are generated at the electrode.[17] The occurrence of an increase of all the ΔE using [Na][BArF] instead of $[Bu_4N][PF_6]$ in dichloromethane indicates the existence of some through space electrostatic contributions in the ΔE values (Table 2). The increase of the ΔE values is smallest on the $\Delta E(E^2 - E^1)$ compared to the other ΔE values, showing that the electrostatic tuning window of the potential differences (ΔE) is larger in the case of the oxidation of already charged species due to the very low ion pairing properties of $[BArF]^-$ in dichloromethane.

Table 2. ΔE in mV measured for **Mo$_2$Flu** and **Mo$_2$bbdt** with [Bu$_4$N][PF$_6$] and [Na][BArF]

Complex/electrolyte	$E^2 - E^1$	$E^3 - E^2$	$E^4 - E^3$
Mo$_2$Flu/[Bu$_4$N][PF$_6$]	80	690	-
Mo$_2$Flu/[Na][BArF]	130	1000	235
Mo$_2$bbdt/[Bu$_4$N][PF$_6$]	120	650	-
Mo$_2$bbdt/[Na][BArF]	200	890	370

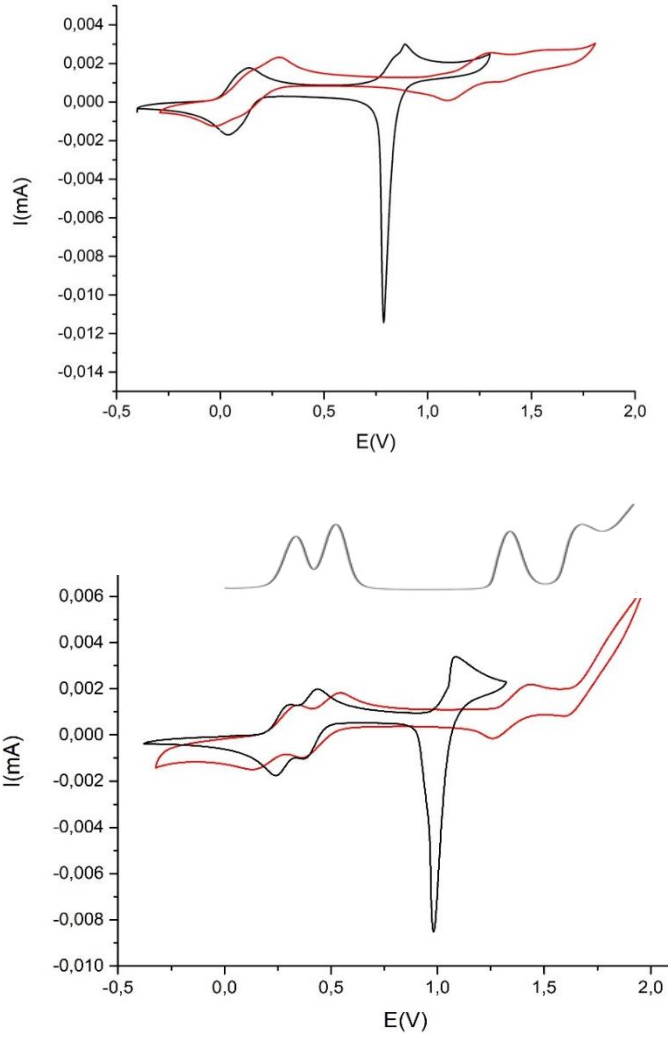

Fig. 4. Cyclic voltammograms of (top) **Mo$_2$Flu** and (bottom) **Mo$_2$bbdt** and DPV (5mV/s) in CH_2Cl_2-Na[B($C_6H_4(CF_3)_2)_4$] 0.02 M (red) in CH_2Cl_2-[NBu_4][PF_6] 0.1 M (black), E in V *vs*. SCE, 100 mV.s^{-1}

2.4.Spectroelectrochemical investigations.

UV−vis−NIR spectroelectrochemical investigations were carried out on freshly prepared **Mo_2Flu** in order to get more insights into the formation and the spectroscopic signature of the various oxidized species and also on the electronic coupling contribution to the ΔE ($E^2 – E^1$) value. This was performed on a dichloromethane solution of the complex containing Bu_4NPF_6 as the supporting electrolyte. The neutral complex exhibits absorption bands only in the UV-vis range at λ_{max} = 324 and 406 nm, close to those observed for the analogous complexes, **Mo_2bbdt** and **$Mo_2$1,4Ph**.[11] The lowest energy absorption band in these neutral complexes is classically assigned to a ligand-to-metal charge transfer (LMCT).[15,18] As can be seen on the differential UV−vis−NIR absorption spectra (Fig. 5), upon gradual oxidation to the mono-oxidized species, the growth of several new absorption bands in the UV-vis region is observed at 346, 496 and 774 nm together with a broad band centered at 1290 nm in the NIR region. This latter band is located at a notably higher wavelength than that generally observed for a single cation radical generated for a mononuclear Cp_2Mo(dithiolene) complex (1040-1150 nm).[11,14,19] According to our previous work, this absorption band centered at 1290 nm is ascribed to an intervalence charge transfer (IVCT) due to the formation of a mixed-valence species. This band in the near IR region indicates an electronic coupling between the two electrophores along the organic linker. This is in line with an electronic delocalization of the unpaired electron in the mixed valence state. This is confirmed by the calculated distribution of the spin density in the mixed valence state (theoretical calculations *vide infra*). Note however, that this band in **$Mo_2Flu^{+\bullet}$** (1290 nm) is observed at higher energy than that of **Mo_2bbdt** (1596 nm)[11], indicating weaker electronic interactions through this fluorene linker.[20] This is in good agreement with the potential separation observed on the CVs between the first two oxidations. Then upon further oxidation to the bis(cation radical) species, the shape of the NIR absorption band changes as it sharpens and shifts at higher energy (1160 nm), where cation radicals of mononuclear

Cp_2Mo(dithiolene) species usually absorbs, suggesting that the bisoxidized state in **Mo_2Flu** is best described as two weakly interacting cation radical species.

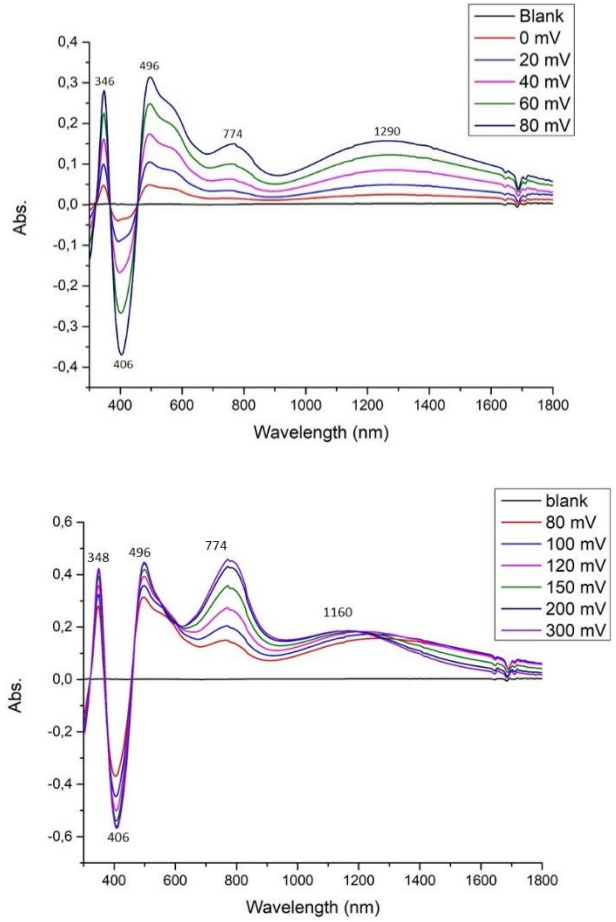

Fig. 5. Differential UV−vis−NIR absorption spectra of the complex **Mo_2Flu** monitored from the neutral state to the monocation radical state upon electrochemical oxidation from 0 to 0.08 V (top) and to the bis(cation radical) state upon electrochemical oxidation from 0.08 to 0.3 V (bottom) in CH_2Cl_2-[NBu_4][PF_6] 0.2 M.

2.5. Theoretical calculations.

DFT computational studies were performed to gain deeper insight into the electronic structure of the neutral molecule and its oxidized species. Geometry optimizations were carried out on a model of the complex using the same base and functional used earlier for **$Mo_2$1,4-Ph** and **Mo_2bbdt**, i.e. Gaussian09, B3LYP/LanL2DZ.[11] In addition, we also performed similar

calculations on the model complex with a biphenyl linker, **Mo$_2$1,4-bPh**, in order to study the influence of the non-rigid biphenyl unit compared to the fluorenyl one. The energy and the nature of the frontier molecular orbitals of **Mo$_2$Flu**, **Mo$_2$1,4-Ph** and **Mo$_2$1,4-bPh** are given in Figure 6. The HOMO of **Mo$_2$Flu** is delocalized over the whole bridging ligand with comparatively little Cp_2Mo contribution. The nature of the HOMO is similar for both complexes with either a fluorenyl or a biphenyl linker. The LUMO is more centered on the Cp_2Mo fragment (Fig. 6). The calculated energy level for the HOMO in **Mo$_2$Flu** (−4.36 eV) is lower in energy in comparison to that of the HOMO in **Mo$_2$1,4-Ph** (−4.27 eV), in accordance with the trend observed for the first redox potential E^1 determined by cyclic voltammetry. The presence of the non-rigid biphenyl linker in the model compound **Mo$_2$1,4-bPh** leads to a HOMO level (−4.42 eV) slightly lower than that of **Mo$_2$Flu** (−4.36 eV).

The MoS_2C_2 metallacycles in the **Mo$_2$Flu** complex are not coplanar with the fluorene moiety but exhibit a dihedral angle between the C_2S_2 planes and the fluorene core of 31°. Similarly, in the biphenyl model, **Mo$_2$1,4-bPh**, a dihedral angle of 28° is observed between the metallacycles and the adjacent phenyl ring. This distortion from planarity is reminiscent to that observed in the optimized geometry of **Mo$_2$1,4-Ph** (24° between the C_2S_2 planes and the phenyl ring). These computed values are in relatively good agreement with those determined by X-ray crystallography for **Mo$_2$1,4-Ph**: 28.9° and 26.7° respectively.[11] With the biphenyl linker, as the two phenyl rings are not constrained to lie in the same plane as with the fluorene, a computed dihedral angle of 31° can be measured between the two phenyl rings plane. The presence of an additional phenyl ring between the two dithiolene moieties does not modify significantly the HOMO-LUMO gap between **Mo$_2$Flu** (2.3 eV) and **Mo$_2$1,4-bPh** (2.35 eV), when compared with that of **Mo$_2$1,4-Ph** (2.26 eV) (Fig. 6).

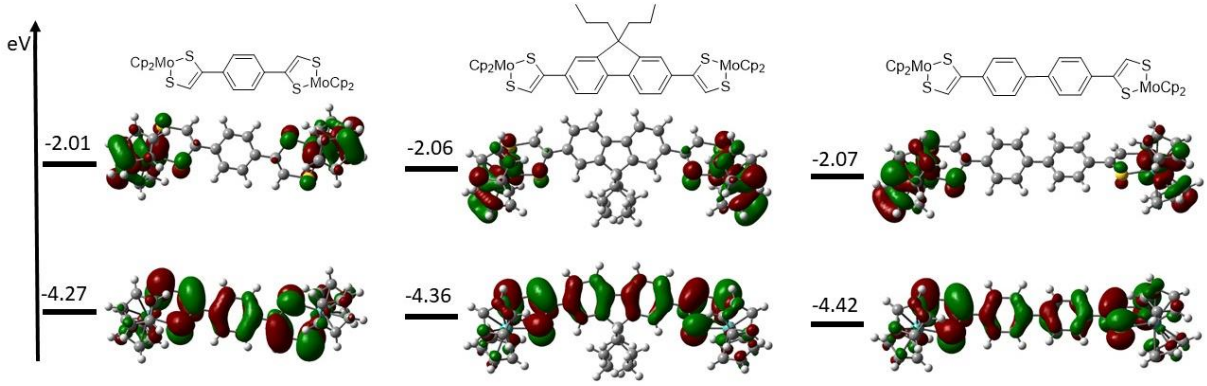

Fig. 6. Frontier molecular orbitals (HOMO and LUMO) and calculated energy levels for complexes **Mo$_2$1,4-Ph** (left), **Mo$_2$Flu** (middle) and model compound **Mo$_2$1,4-bPh** (right) shown with a cutoff of 0.04 [e/bohr^3]$^{1/2}$.

The Mo•••Mo distance in the optimized geometry of the neutral complexes **Mo$_2$1,4-Ph** and **Mo$_2$bbdt** is 12.65 and 12.75 Å respectively, while, as expected, it is significantly longer in **Mo$_2$Flu** and **Mo$_2$1,4-bPh**: 16.06 Å and 16.79 Å (Fig. S3, SI). The presence of one additional aromatic ring in the organic linker, fluorenyl in **Mo$_2$Flu**, significantly lengthens the distance between the two redox active Cp_2Mo(dithiolene) moieties by about 4 Å compared with **Mo$_2$1,4-Ph** and **Mo$_2$bbdt** and even more with the non-rigid biphenyl linker.

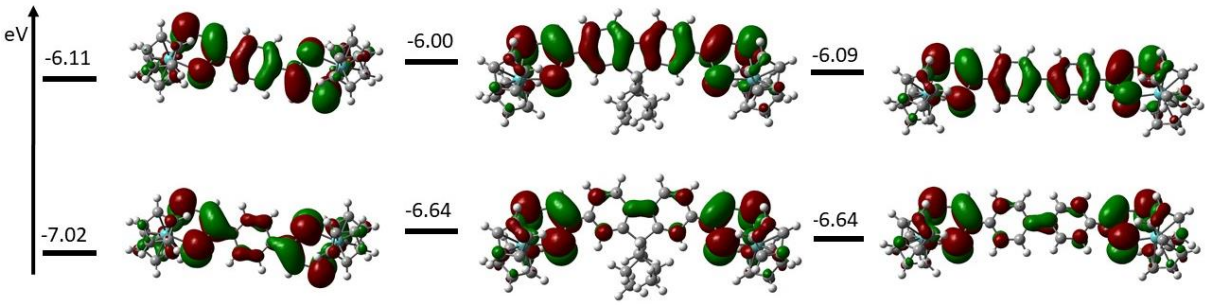

Fig. 7. Frontier molecular orbitals (SOMO and LUMO) and calculated energy levels for complexes **Mo$_2$1,4-Ph$^{+\bullet}$** (left), **Mo$_2$Flu$^{+\bullet}$** (middle) and **Mo$_2$1,4-bPh$^{+\bullet}$** (right) shown with a cutoff of 0.04 [e/bohr^3]$^{1/2}$.

In the radical cation state, the SOMO is essentially localized on the bis(dithiolene) ligand with a lower contribution on the central fluorene core (Fig. 7). A smaller dihedral angle between the dithiolene moieties and the central aromatic core is observed: 20° for **Mo$_2$Flu**$^{+\bullet}$ and 18.3° for **Mo$_2$1,4-bPh**$^{+\bullet}$. This tendency of planarization upon oxidation is also observed between the two phenyl rings of **Mo$_2$1,4-bPh**$^{+\bullet}$: 23° *vs* 31° in the neutral state. The energy levels of the SOMO for **Mo$_2$Flu**$^{+\bullet}$ (−6.64 eV) and **Mo$_2$1,4-bPh**$^{+\bullet}$ (−6.64 eV), at higher energies than the SOMO of **Mo$_2$1,4-Ph**$^{+\bullet}$ (−7.02 eV) is also in accordance with the trend observed for the redox potentials for **Mo$_2$Flu**. Finally, small differences in the calculated spin density of the two mono-oxidized species **Mo$_2$Flu**$^{+\bullet}$ and **Mo$_2$1,4-bPh**$^{+\bullet}$ are found. The spin density contribution on the organic linker is relatively smaller in **Mo$_2$1,4-bPh**$^{+\bullet}$ compared with **Mo$_2$Flu**$^{+\bullet}$ (Fig. 8).

We resorted to compare the outcome of the theoretical calculations on the complexes **Mo$_2$1,4-bPh** and **Mo$_2$Flu** with similar Mo•••Mo distances but with organic linkers of different rigidity. Despite its slightly distorted structure, **Mo$_2$1,4-bPh** retains a non-negligible amount of electronic coupling, even if smaller than that found in **Mo$_2$Flu** with the rigid fluorene linker. Concomitantly, comparable through-space electrostatic interactions are expected in both complexes since the Mo•••Mo distances are very close. As observed for other bis redox active complexes with a biphenyl organic linker,[21] here the presence of a fluorenyl linker which is a more rigid planar biphenyl unit still allows for some electronic interactions. These electronic interactions are weaker due to the longer organic linker, (Mo-Mo distance = 16.06 Å, *vide infra*), compared with the complex with one phenyl ring **Mo$_2$1,4P** (Mo-Mo distance = 12.65 Å).

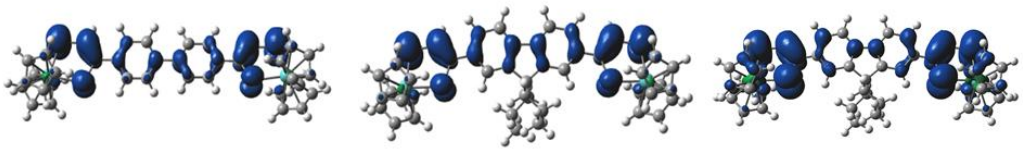

Fig. 8. Spin density of **Mo$_2$1,4bP$^{+\bullet}$** (left), **Mo$_2$Flu$^{+\bullet}$** (middle) and **Mo$_2$Flu$^{2(+\bullet)}$** shown with a cutoff of 0.001 e/bohr^3.

Finally we also performed DFT calculations on the bis oxidized state of **Mo$_2$Flu** (Fig S4) in order to evaluate which spin state, singlet or triplet, is the most stable one. A strong electronic delocalization in the dication should be consistent with a singlet state while essentially independent monocationic Cp$_2$Mo(dithiolene)$^{+\bullet}$ moieties should stabilize the triplet state. It appears that the triplet state in **Mo$_2$Flu**$^{2+}$ is more stable by 0.92 eV than the singlet one. The spin density contribution is now essentially located on the dithiolene moieties with a small contribution on the fluorenyl spacer. This finding is in agreement with the energy of the absorption band of the dicationic species found at a wavelength (1160 nm) similar to that observed for mononuclear [Cp$_2$Mo(dithiolene)]$^{+\bullet}$ radical cations (1040-1150nm).[11,14,19] Thus, in **Mo$_2$Flu$^{2(+\bullet)}$**, each cation radical species is essentially localized on the Cp$_2$Mo(dithiolene) moeties. In order to confirm this hypothesis we chemically generated the bisoxidized species. This was performed by adding two equivalent of [Cp$_2$Fe][BF$_4$] to a dichloromethane solution of **Mo$_2$Flu** under inert atmosphere. The bisoxidized species precipitated in the medium after the addition of pentane. The UV-vis-NIR absorption spectrum of this precipitate redissolved in CH_2Cl_2 shows a broad band located at 1150 nm in accordance with the spectroscopic signature obtained for the bisoxidized species during the spectroelectrochemical experiment. Moreover, the EPR spectrum of a dichloromethane solution of this precipitate at room temperature displays an isotropic signal at g_{iso} of 2.013 which indicates an organic radical character (Fig. 9). This spectrum shows hyperfine splitting due to coupling of the unpaired electron spin with one hydrogen atom of the dithiolene metallacycle and with the molybdenum center ^{95}Mo and ^{97}Mo

isotopes (25.5%, I = 5/2). This observation is consistent with the significant spin density found on each dithiolene moieties by theoretical calculation of and confirmed the stable triplet state of the bisoxidized species, **$Mo_2Flu^{2(+\bullet)}$** with two weakly coupled mono-oxidized electrophores.

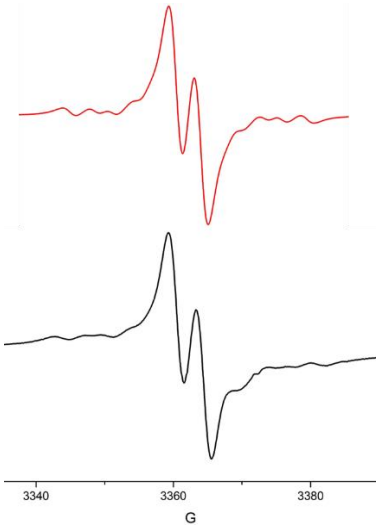

Fig. 9. EPR spectrum of **$Mo_2Flu^{2(+\bullet)}$** recorded in CH_2Cl_2 at room temperature (black line). Simulated spectrum (red line) with g_{iso}= 2.0134, A_{Mo}= 3.68 10^{-4} cm^{-1} and a_H= 3.74 10^{-4} cm^{-1} created using a Lorentzian line shape and a 2.60 G line width.

3. Conclusion

In summary, we have presented here a chemical route for the synthesis of an original electroactive bis[Cp_2Mo(dithiolene)] complex where the two dithiolene moieties are separated by a fluorene linker. We have shown through electrochemical investigations using traditional and weakly coordinating supporting electrolytes the existence of through space electrostatic interactions between the two metallacycles. Indeed, the two closely spaced first oxidation steps of the **Mo_2Flu** complex shift from a ΔE value of 80 mV with [Bu_4N][PF_6] to a ΔE of 130 mV with [Na][BArF] in dichloromethane. The extent of electronic coupling in the complex has been analyzed through spectroelectochemical studies and DFT calculations, indicating that the spin density in the radical cation state is delocalized over the two electrophores and the organic

linker. The electronic interaction in the mixed valence state can be experimentally measured, although of lower magnitude than in its congeners with a shorter intermetallic distance (12 vs 16 Å), and has been shown to comprise substantial through-bond and through space interactions. Finally the bis(oxidized) complex can be described as a stable triplet state with localized bis cation radical species.

4. Experimental section

4.1.General.

Chemicals and materials from commercial sources were used without further purification. All the reactions were performed under an argon atmosphere. The synthesis of **Mo_2Fl** was carried out by using Schlenk techniques and vacuum-line systems under an argon atmosphere. Melting points were measured on a Kofler hot-stage apparatus and are uncorrected. Mass spectra were recorded by the Centre Régional de Mesures Physiques de l'Ouest, Rennes. Methanol and dichloromethane were dried using Inert pure solvent column device. CVs and DPVs were carried out on a 10^{-3} M solution of complex in CH_2Cl_2 with NBu_4PF_6 0.1 M, or, when specified, with ca. 0.02 M NaBARF. NaBARF or $[Na][B(C_6H_4(CF_3)_2)_4]$ is Sodium tetrakis[3,5-bis(trifluoromethyl)phenyl]borate. Potentials were measured versus the Saturated Calomel Electrode (SCE). DPV were measured with P_H = 25 mV and S_H = 5 mV (P_H : Pulses height and S_H : Step height). Deconvolution of the first oxidation wave to two independent redox systems was performed by using the software "Magic Plot". Compound **1** was prepared according to a literature procedure.[22] X-band EPR spectra were recorded on a Bruker EMX spectrometer and simulated using WINEPR SimFonia, Shareware version 1.25, Brüker Analytische Messtechnik GmbH.

4.2.Synthesis and characterization

Synthesis of 1,1'-(9,9-dipropyl-9H-fluorene-2,7-diyl)bis(ethan-1-one) 2: to an ice-cooled solution of 9,9-dipropylfluorene **1** (4.63 g, 18.52 mmol) in dry dichloromethane (30 mL) under argon atmosphere was added dropwise a solution of $AlCl_3$ (7.4 g, 55.56 mmol) and acetyl chloride (3.9 mL, 55.56 mmol) in dry dichloromethane (30 mL) (Friedel-Crafts conditions). The reaction mixture was stirred overnight at room temperature. After that the reaction mixture was washed with water and dried with $MgSO_4$. After evaporation of the solvent, the product precipitated with the addition of methanol. The precipitate was collected by filtration and dried to produce compound **2** as a yellow solid. (4.45 g, 13.3 mmol) in 72 % yield. Crystals of sufficient quality for X-ray diffraction were obtained by slow evaporation of a dichloromethane solution. mp 166 °C; ^{1}H NMR (300 MHz, $CDCl_3$) δ 7.99 – 7.96 (m, 4H), 7.86 – 7.81 (m, 2H), 2.68 (s, 6H), 2.06 – 2.01 (m, 4H), 0.67-0.59 (m, 10H); ^{13}C NMR (75 MHz, $CDCl_3$) δ 197.97, 152.30, 144.43, 136.88, 128.22, 122.57, 120.53, 55.81, 42.32, 26.87, 17.16, 14.29; IR : $\tilde{\nu}_{CO}$ = 1681 cm^{-1}; HRMS (ESI) calcd for $C_{23}H_{26}O_2$ [$M^{+\cdot}$] 334.1938, found 334.1929. Anal. Calcd for [$C_{23}H_{26}O_2$]: C, 82.60; H, 7.84. Found: C, 82.63; H, 8.05.

Synthesis of 1,1'-(9,9-dipropyl-9H-fluorene-2,7-diyl)bis(2-bromoethan-1-one) 3 : 1,1'-(9,9-dipropyl-9H-fluorene-2,7-diyl)bis(ethan-1-one) **2** (2 g, 6 mmol) was dissolved in acetic acid (60 mL), then bromine (1.91 g, 12 mmol) was added slowly. After addition, the reaction mixture was heated to 50 °C for 20 min. The reaction mixture poured into iced water and the precipitate was filtered off and washed with water and dried overnight. Purification by flash chromatography using dichloromethane / petroleum ether(1/1) (Rf = 0.5) afforded the product as a white solid (2 g, 4 mmol). Crystals of sufficient quality for X-ray diffraction were obtained

by slow evaporation of a dichloromethane solution: Yield 67%; mp 137 °C; ^{1}H NMR (300 MHz, $CDCl_3$) δ 8.06 – 7.97 (m, 4H), 7.91 – 7.80 (m, 2H), 4.52 (s, 4H), 2.04 (dd, *J* = 9.6, 6.0 Hz, 4H), 0.72 – 0.50 (m, 10H); ^{13}C NMR (75 MHz, $CDCl_3$) δ 191.25, 152.71, 145.02, 133.57, 128.80, 123.61, 121.07, 56.03, 42.26, 31.16, 17.29, 14.37; UV-vis (CH_2Cl_2) λ (nm) (ε [$L.mol^{-1}cm^{-1}$]) 340 (18800), 315 (13600); IR : $\tilde{\nu}_{CO}$ = 1696 cm^{-1}; HRMS (ESI) calcd for $C_{23}H_{24}O_2$ [$M^{+\cdot}$] 490.0137, found 490.0142 Anal. Calcd for [$C_{25}H_{22}O_2Br_2$]: C, 56.12; H, 4.91. Found: C, 56.12; H, 5.03.

Synthesis of 4,4'-(9,9-dipropyl-9H-fluorene-2,7-diyl)bis(1,3-dithiol-2-one) 4 : To a solution of 1,1'-(9,9-dipropyl-9H-fluorene-2,7-diyl)bis(2-bromoethan-1-one) **3** (2.4 g, 4.87 mmol) in 100 mL dichloromethane, potassium isopropyl xanthate (2.55 g, 14.6 mmol) was added and the reaction mixture was refluxed overnight. Filtration through celite and evaporation of the solvent afforded a yellow solid with quantitative yield (2.93 g) which was used without further purification: ^{1}H NMR (300 MHz, $CDCl_3$) δ 8.07 (dd, *J* = 7.6, 1.4 Hz, 4H), 7.91 – 7.83 (m, 2H), 5.74 (hept, *J* = 6.2 Hz, 2H), 4.71 (s, 4H), 2.05 (t, *J* = 7.6 Hz, 4H), 1.38 (d, *J* = 6.2 Hz, 12H), 0.64 (t, *J* = 7.3 Hz, 10H); ^{13}C NMR (75 MHz, $CDCl_3$) δ 212.23, 192.20, 152.28, 144.55, 135.34, 127.99, 122.80, 120.58, 78.76, 55.71, 43.08, 41.97, 20.95, 16.93, 14.06. Then the compound (1.2 g, 2 mmol) was dissolved in 50 mL of chloroform and 1.5 mL perchloric acid was added. The reaction mixture was stirred for 8 h at 70°C. The reaction mixture was allowed to reach room temperature and water was added. The organic phase was washed with $NaHCO_3$ then water and dried over $MgSO_4$. Evaporation of the solvent afforded a yellow solid (0.911 g, 1.9 mmol) in 95 % Yield. Crystals of sufficient quality for X-ray diffraction were obtained by slow evaporation of a dichloromethane solution: mp 240 °C; ^{1}H NMR (300 MHz, $CDCl_3$) δ 7.72 (d, *J* = 6 Hz, 2H), 7.42 (d, *J* = 6 Hz, 2H), 7.39 (s, 2H), 6.91 (s, 2H), 2.01-1.96 (m, 4H), 0.69-0.65 (m, 10H); ^{13}C NMR (75 MHz, $CDCl_3$) δ 191.9, 151.8, 140.8, 135.0, 131.8, 125.4, 120.4, 120.3,

111.2, 55.5, 42.3, 16.9, 14.1; UV-vis (CH_2Cl_2) λ (nm) (ε [$L.mol^{-1}cm^{-1}$]) 348 (37000), 235 (15800); IR : $\tilde{\nu}_{CO}$ = 1634 cm^{-1}; HRMS (ESI) calcd for $C_{23}H_{24}O_2$ [$M^{+\cdot}$] 482.05027, found 482.0499; Anal. Calcd for [$C_{25}H_{22}O_2S_4$]: C, 62.61; H, 4.59; S, 26.57. found: C, 62.69; H, 5.05; S, 26.64.

Synthesis of Mo_2Flu : In a Schlenk containing the proligand **4** (240 mg, 0.5 mmol) dissolved in dry THF(10 mL) under an inert atmosphere, a solution of NaOMe (freshly prepared from sodium (60 mg, 2.6 mmol) in 10 mL of dry methanol was added. The reaction mixture was stirred for 2 h at 45 °C, then cooled to room temperature and Cp_2MoCl_2 (295 mg, 1 mmol) was added. The reaction mixture was stirred overnight at 60 °C. After evaporation of the solvent, dichloromethane was added and the organic layer was washed with degassed water then the water was removed via cannula and the product was dried under vacuum. After slow diffusion (CH_2Cl_2/pentane), compound **Mo_2Fl** was obtained as a brown powder (361 mg, 0.41 mmol). Yield 82%; ^{1}H NMR (400 MHz, $CDCl_3$) δ 7.65 (d, *J* = 6.1 Hz, 2H), 7.59 (m, 2H), 7.48 (d, *J* = 6.1 Hz, 2H), 6.85 (s, 2H), 5.30 (s, 20H), 1.90 (m, 4H), 1.28 (m, 4H), 0.67 (m, 6H); ^{13}C NMR (101 MHz, $CDCl_3$) δ 150.4, 138.4, 124.6, 120.1, 118.3, 98.1, 67.7, 54.8, 42.5, 25.3, 16.9, 14.3; UV-vis (CH_2Cl_2) λ (nm) (ε [$L.mol^{-1}cm^{-1}$]) 324 (24120) and 406 (12080) nm; HRMS (ESI) calcd for $C_{43}H_{38}S_4Mo_2$ [$M^{+\cdot}$] 882.02775**,** found 882.028(1 ppm).

4.3. Crystallography

Suitable crystals of **2**, **3** and **4** for X-ray diffraction single crystal experiment were selected and mounted with a cryoloop on the goniometer head of a D8 VENTURE Bruker AXS diffractometer, diffractometer equipped with a (CMOS) Photon 100 detector, using Mo-Kα radiation (λ = 0.71073

Å, multilayer monochromator). The structures were solved by dual-space algorithm using the *SHELXT* program,[23] and the refined with full-matrix least-square methods based on F^2 (*SHELXL*).[24] All non-hydrogen atoms were refined with anisotropic atomic displacement parameters. H atoms were finally included in their calculated positions. Crystallographic data on X-ray data collection and structure refinements are given in Table 3. CCDC 2150926-2150928 for compounds **2**, **3** and **4** respectively.

Table 3 Crystallographic data

Compound	**2**	**3**	**4**
Formula	$C_{23}H_{26}O_2$	$2(C_{23}H_{24}Br_2O_2),CH_2Cl_2$	$C_{23}H_{26}O_2$
FW ($g\cdot mol^{-1}$)	334.44	1069.41	482.66
Crystal system	monoclinic	monoclinic	monoclinic
Space group	*C* 2/*c*	*P* 2_1/*n*	*P* 2_1/*n*
a (Å)	12.7471(11)	15.0805(7)	7.8702(5)
b (Å)	10.4097(10)	8.9063(5)	12.3606(7)
c (Å)	28.529(3)	32.8144(17)	23.5448(12)
α (°)	90	90	90
β (°)	94.458(3)	96.116(2)	98.379(2)
γ (°)	90	90	90
V ($Å^3$)	3774.1(6)	4382.3(4)	2266.0(2)
T (K)	150(2)	150(2)	150(2)
Z	8	4	4
D_{calc} ($g\cdot cm^{-3}$)	1.777	1.621	1.415
μ (mm^{-1})	0.073	3.839	0.440
Total refls.	14153	35524	17145
Abs. Corr .	multi-scan	multi-scan	multi-scan
Uniq. refls. (R_{int})	4161 (0.0723)	9977(0.0505)	5127(0.0355)
Unique refls. ($I > 2\sigma(I)$)	3302	8008	4373
R_1, wR_2	0.0685, 0.1766	0.0524, 0.1178	0.0581, 0.1388
R_1, wR_2 (all data)	0.0868, 0.1898	0.0699, 0.1258	0.0680, 0.1446
GoF	1.036	1.025	1.070

4.4 DFT Calculations

Full geometry optimization of neutral and charged complexes were performed with Density Functional Theory[25] using the hybrid Becke-3 parameter exchange functional[26] and the Lee-Yang-Parr nonlocal correlation functional[27] (B3LYP) implemented in the the Gaussian 09 Revision D.01 software suite (or later releases) and using the LANL2DZ basis set.[28] GaussView 5.0.9 was used to generate the figures.

Author contributions

Conceptualization and designed experiments: D. L. Experimental synthetic work and cyclic voltammetry experiments performed by K. Y. Spectroelectrochemical experiments carried out by A. V. Theoretical calculations performed by F. B. X-Ray crystallography investigation: T. R. Writing, review and editing: D. L, F. B., and A. V. All authors have approved the final draft of the manuscript.

Conflict of interest

There are no conflict of interest to declare

Appendix A.

Supplementary data CCDC 2150926-2150928 contains the supplementary crystallographic data for compounds **2**, **3** and **4** respectively. These data can be obtained free of charge via http://www.ccdc.cam.ac.uk/conts/retrieving.html, or from the Cambridge Crystallographic Data Centre, 12 Union Road, Cambridge CB2 1EZ, UK; fax: (+44) 1223-336-033; or e-mail: deposit@ccdc.cam.ac.uk.

Acknowledgements

Financial support was obtained from ANR (Paris France) under contract n°19-CE08-0029-02. This work was granted access to the HPC resources of CINES under the allocation 2021-A0100805032 awarded by GENCI.

Supplementary material

Electronic supplementary information (ESI) available. CCDC 2150926-2150928 and Molecular structures of compounds **2** and **3**. For ESI and crystallographic data in CIF or other electronic format see DOI:

References

[1] Dithiolene Chemistry, Prog. Inorg. Chem., E. I. Stiefel Ed. 2004, vol. 52

[2] (a) R. Eisenberg and H. Gray, Noninnocence in metal complexes: a dithiolene dawn, Inorg. Chem. 50 (2011) 9741-9751. (b) G. Periyasamy, N. A. Burton, I. H. Hillier, M. A. Vincent, H. Disley, J. McMaster and C. D. Garner, The dithioleneligand—'innocent' or 'non-innocent'? A theoretical and experimental study of some cobalt–dithiolene complexes, Faraday Discuss. 135 (2007) 469–488.

[3] R. Sakamoto, K. Takata, T. Pal, H. Maeda, T. Kambe and H. Nishihara, Coordination nanosheets (CONASHs): strategies, structures and functions, Chem. Commun. 53 (2017) 5781-5801.

[4] W. Shi, G. Wu, K. Hippalgaonkar, J.-S. Wang, J. Xu and S.-W. Yang, Poly(nickel-ethylenetetrathiolate) and its analogs: Theoretical prediction of high-performance doping-free thermoelectric polymers, J. Am. Chem. Soc. 140 (2018) 13200-13204.

[5] (a) T. Kambe, R. Sakamoto, K. Hoshiko, K. Takada, M. Miyachi, J.-H. Ryu, S. Sasaki, J. Kim, K. Nakazato, M. Takata and H. Nishihara, π-Conjugated nickel bis(dithiolene) complex nanosheet, J. Am. Chem. Soc. 135 (2013) 2462-2465. (b) T. Kambe, R. Sakamoto, T. Kusamoto, T. Pal, N. Fukui, K. Hoshiko, T. Shimojima, Z. Wang, T. Hirahara, K. Ishizaka, S. Hasegawa, F. Liu and H. Nishihara, Redox control and high conductivity of nickel bis(dithiolene) complex π-nanosheet: A potential organic two-dimensional topological

insulator, J. Am. Chem. Soc. 136 (2014) 14357-14360. (c) X. Huang, H. Li, Z. Tu, L. Liu, X. Wu, J. Chen, Y. Liang, Y Zou, Y. Yi, J. Sun, W. Xu and D. Zhu, Highly conducting neutral coordination polymer with infinite two-dimensional silver-sulfur networks, J. Am. Chem. Soc. 140 (2018) 15153-15156.

[6] (a) A. J. Clough, N. M. Orchanian, J. M. Skelton, A. J. Neer, S. A. Howard, C. A. Downes, L. F. J. Piper, A. Walsh, B. C. Melot and S. C. Marinescu, Room temperature metallic conductivity in a metal–organic framework induced by oxidation, J. Am. Chem. Soc. 141 (2019) 16323−16330. (b) A. J. Clough, J. M. Skelton, C. A. Downes, A. A. de la Rosa, J. W. Yoo, A. Walsh, B. C. Melot and S. C. Marinescu, Metallic conductivity in a two-dimensional cobalt dithiolene metal–organic framework, J. Am. Chem. Soc. 139 (2017) 10863-10867.

[7] H. Banda, J.-H. Dou, T. Chen, N. J. Libretto, M. Chaudhary, G. M. Bernard, J. T. Miller, V. K. Michaelis and M. Dinca, Signature of metallic behavior in the metal-organic frameworks M_3(hexaiminobenzene)$_2$ (M = Ni, Cu), J. Am. Chem. Soc. 139 (2017) 2285-2292.

[8] J. Cui and Z. Xu, An electroactive porous network from covalent metal–dithiolene links, Chem. Commun. 50 (2014) 3986-3988

[9] (a) J. J. Maj, A.D. Rae and L. F. Dahl, Transition metal-promoted carbon-carbon bond formation by reductive dimerization of carbon disulfide: direct synthesis of the bis(1,2-dithiolene-like) tetrathiooxalato (C_2S_4) ligand from carbon disulfide by reaction with the dimeric nickel(I) complexes $Ni_2(\eta^5\text{-}C_5R_5)_2(\mu\text{-}CO)_2$ (R = H, Me), J. Am. Chem. Soc. 104 (1982) 4278-4280. (b) R. Vicente, J. Ribas, P. Cassoux and L. Valade, Synthesis, characterization and properties of highly conducting organometallic polymers derived from the ethylene tetrathiolate anion, Synthetic Metals, 13 (1986) 265-280. (c) R. Vicente, J. Ribas, S. Alvarez, A. Segui, X. Solans and M. Verdaguer, Synthesis, x-ray diffraction structure, magnetic properties, and MO analysis of a binuclear (μ-tetrathiooxalato)copper(II) complex, $(AsPh_4)_2[(C_3OS_4)CuC_2S_4Cu(C_3OS_4)]$, Inorg. Chem. 26 (1987) 4004-4009. (d) A. E. Pullen, S.

Zeltner, R. M. Olk, E. Hoyer, K. A. Abboud and J. R. Reynolds, Extensively conjugated dianionic tetrathiooxalate-bridged copper(II) complexes for synthetic metals, Inorg. Chem. 35 (1996) 4420-4426. (e) M. Hayashi, K. Otsubo, T. Kato, K. Sugimoto, A. Fujiwara and H. Kitagawa, A compact planar low-energy-gap molecule with a donor–acceptor–donor nature based on a bimetal dithiolene complex, Chem. Commun. 51 (2015) 15796-15799.

[10] (a) H. Köpf and H. Balz, Benzol-1,2,4,5-tetrathiolato-zweikernkomplexe des titanocen-, zirconocen- und hafnocen-systems, J. Organomet. Chem. 387 (1990) 77-81. (b) H. Balz, H. Köpf and J. Pickardt, Benzol-1,2,4,5-tetrathiolato-zweikernkomplexe der 1,1′-bis(trimethylsilyl)metallocene der titantriade—synthese und strukturbestimmung von [(η5-$Me_3SiC_5H_4)_2TiS_2]_2C_6H_2$ und [(η^5-$Me_3SiC_5H_4)_2HfS_2]_2C_6H_2$, J. Organomet. Chem. 417 (1991) 397-406. (c) K. Arumugam, M. C. Shaw, P. Chandrasekaran, D. Villagrán, T. G. Gray, J. T. Mague and J. P. Donahue, Synthesis, structures, and properties of 1,2,4,5-benzenetetrathiolate linked group 10 metal complexes, Inorg. Chem. 48 (2009) 10591-10607.

[11] A. Vacher, Y. Le Gal, T. Roisnel, V. Dorcet, T. Devic, F. Barrière and D. Lorcy, Electronic communication within flexible bisdithiolene ligands bridging molybdenum centers, Organometallics, 38 (2019) 4399-4408.

[12] N. Svenstrup and J. Becher, The organic chemistry of 1,3-dithiole-2-thione-4,5-dthiolate(dmit) Synthesis, (1995) 215-235.

[13] P. Hapiot, C. Lagrost, F. Le Floch, E. Raoult and J. Rault-Berthelot, Comparative study of the oxidation of fluorene and 9,9-disubstituted fluorenes and their related 2,7‘-dimers and trimer, Chem. Mater. 17 (2005) 2003–2012.

[14] A. L.Whalley, A. J. Blake, D. Collison, E. S. Davie, H. J. Disley, M. Helliwell, F. E. Mabbs, J. McMaster, C. Wilson and C. D. Garner, Synthesis, structure and redox properties of bis(cyclopentadienyl)dithiolene complexes of molybdenum and tungsten, Dalton Trans. 40 (2011) 10457-10472.

[15] A. J. Taylor, E. S. Davies, J. A. Weinstein, I. V. Sazanovich, O. V. Bouganov, S. A. Tikhomirov, M. Towrie, J. McMaster and C. D. Garner, Ultrafast intramolecular charge separation in a donor-acceptor assembly comprising bis(η5-cyclopentadienyl)molybdenum coordinated to an ene-1,2-dithiolate-naphthalenetetracarboxylicdiimide ligand, Inorg. Chem. 51 (2012) 13181-13194.

[16] (a) M. L. H. Green, W. B. Heuer, G. C. Saunders, Synthesis and electrochemistry of crown ether dithiolene complexe, J. Chem. Soc., Dalton Trans. (1990) 3789-3792. (b) M. Fourmigué, C. Lenoir, C. Coulon, F. Guyon, J. Amaudrut, Antiferromagnetic interactions in charge-transfer salts of molybdocene dithiolene complexes: the example of $[Cp_2Mo(dddt)][TCNQ]$, Inorg. Chem. 34 (1995) 4979-4985. (c) I. V. Jourdain, M. Fourmigué, F. Guyon, J. Amaudrut, Syntheses and electrochemical characterization of heteroleptic cyclopentadienyl–dithiolene d^2 tungsten complexes. Structures and magnetic properties of charge-transfer salts, J. Chem. Soc., Dalton Trans. (1998) 483-488.

[17] (a) F. Barrière and W. E. Geiger, Use of Weakly Coordinating Anions to Develop an Integrated Approach to the Tuning of $\Delta E_{1/2}$ Values by Medium Effects, J. Am. Chem. Soc. 128 (2006) 3980-3989. (b) W. E. Geiger and F. Barrière, Organometallic electrochemistry based on electrolytes containing weakly-coordinating fluoroarylborate anions, Acc. Chem. Res. 43 (2010) 1030-1039. (c) F. Barrière, R. J. LeSuer, W. E. Geiger, "Electrochemical advances using fluoroarylborate anion supporting electrolytes" in Trends in Molecular Electrochemistry, Eds.: A. J. L. Pombeiro, C. Amatore Fontis Media, Marcel Dekker, Chapter 13, p. 413-444 (2004). (d) F. Barrière, Electrostatic modeling of the tunable potential difference between the two consecutive oxidation steps of dinickel bisfulvalene, Organometallics 33 (2014) 5046-5048.

[18] J. K. Hsu, C. J. Bonangelino, S. P. Kaiwar, C. M. Boggs, J. C. Fettinger and R. S. Pilato, Direct Conversion of α-Substituted Ketones to Metallo-1,2-enedithiolates, Inorg. Chem. 35 (1996) 4743-4751.

[19] (a) T. Bsaibess, M. Guerro, Y. Le Gal, D. Sarraf, N. Bellec, M. Fourmigué, F. Barrière, V. Dorcet, T. Guizouarn, T. Roisnel and D. Lorcy, Variable magnetic interactions between S = 1/2 cation radical salts of functionalizable electron-rich dithiolene and diselenolene Cp_2Mo complexe, Inorg. Chem. 52 (2013) 2162-2173. (b) Y. Le Gal, T. Roisnel, V. Dorcet, T. Guizouarn, L. Piekara-Sady and D. Lorcy, Chiral electron-rich bis(cyclopentadienyl) dithiolene molybdenum complexes, J. Organomet. Chem. 794 (2015) 323-329.

[20] M. D. Ward and J. A. McCleverty, Non-innocent behaviour in mononuclear and polynuclear complexes: consequences for redox and electronic spectroscopic properties, J. Chem. Soc., Dalton Trans. (2002) 275-288.

[21] D. Osella, L. Milone, C. Nervi and M. Ravera, Electronic Communication in $[Co_2(CO)_6]_2$-diyne and $[Co_2(CO)_4(dppm)]_2$-diyne complexes, Eur. J. Inorg. Chem. (1998) 1473-1477.

[22] E. Cerrada, M. Laguna and N. Lardies, Bis(1,2,3-thiadiazole)s as precursors in the synthesis of bis(alkynethiolate)gold(I) derivatives, Eur. J. Inorg. Chem. (2009) 137-146.

[23] G. M. Sheldrick, SHELXT-Integrated Space-Group and Crystal-Structure Determination, Acta Cryst. A71 (2015) 3-8.

[24] G. M. Sheldrick, Crystal structure refinement with SHELXL, Acta Cryst. C71 (2015) 3-8

[25] (a) P. Hohenberg, W. Kohn, Phys. Rev. 136 (1964) B864. (b) R. G. Parr, W. Yang, *Density-Functional Theory of Atoms and Molecules*; Oxford University Press: Oxford, U.K., 1989

[26] (a) A. D. Becke, Density-functional exchange-energy approximation with correct asymptotic behaviour, Phys. Rev. A 38 (1988) 3098. (b) A. D. Becke, A new mixing of Hartree-Fock and local density-functional theories, J. Chem. Phys. 98 (1993) 1372-1377. (c) A. D. Becke, Density functional thermochemistry. III. The role of exact exchange, J. Chem. Phys. 98 (1993) 5648.

[27] C. Lee, W. Yang, R. G. Parr, Development of the Colle-Salvetti correlation-energy formula into a functional of the electron density, Phys. Rev. B 37 (1988) 785.

[28] (a) W. R. Wadt, P. J. Hay, Ab initio effective core potentials for molecular calculations – potentials for main group elements Na to Bi, J. Chem. Phys. 82 (1985) 284-298. (b) P. J. Hay, W. R. Wadt, Ab initio effective core potentials for molecular calculations. Potentials for K to Au including the outermost core orbitals, J. Chem. Phys. 82 (1985) 299-310.